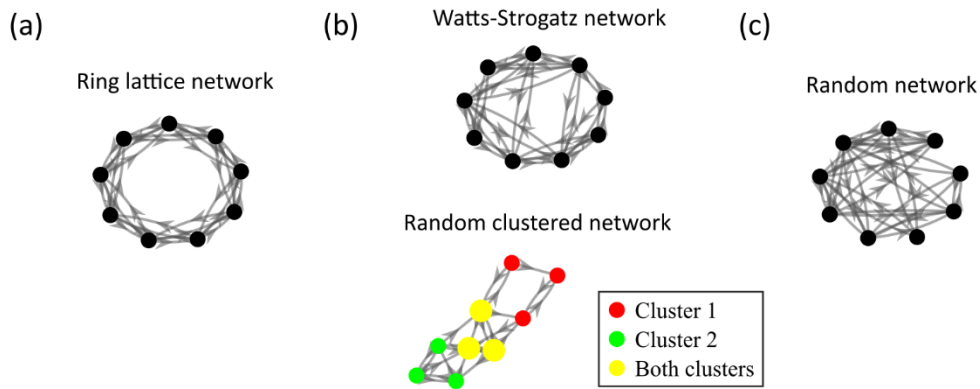


1056 **Supplemental figures**

1057

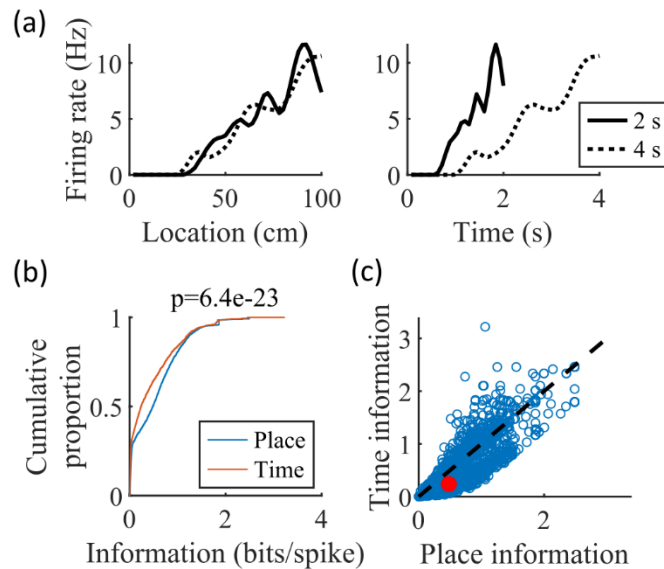


1058 **Figure 1—figure supplement 1: Comparison of the randomly clustered network and**
1059 **the canonical Watts-Strogatz small-world network**

1060 **(a)** A small ring-lattice network. **(b)** Example small-world networks. Top, a Watts-Strogatz
1061 network with re-wiring parameter $\beta = 0.2$. Bottom, a randomly clustered network with
1062 two clusters and a cluster participation of 1.25. **(c)** Example randomly connected network.

1063

1064



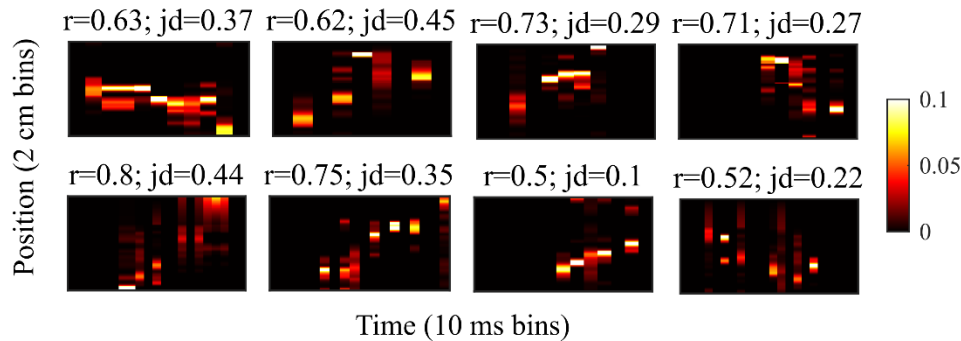
1065 **Figure 3—figure supplement 1: The simulated cells have greater place information**
1066 **than time information.**

1067 **(a)** Place fields (left) and time fields (right) for an example cell calculated from simulated
1068 trajectories that took 2 seconds (solid line) or 4 seconds (dotted line) to traverse the track.

1069 **(b)** CDFs of the information content of the place fields (“Place”) and time fields (“Time”) of
1070 all cells. The spatial information is significantly greater than the temporal information (KS-
1071 test, $p=6.4e-23$). **(c)** Scatter plot of the data in (b), with the median values marked in red.

1072

1073



1074

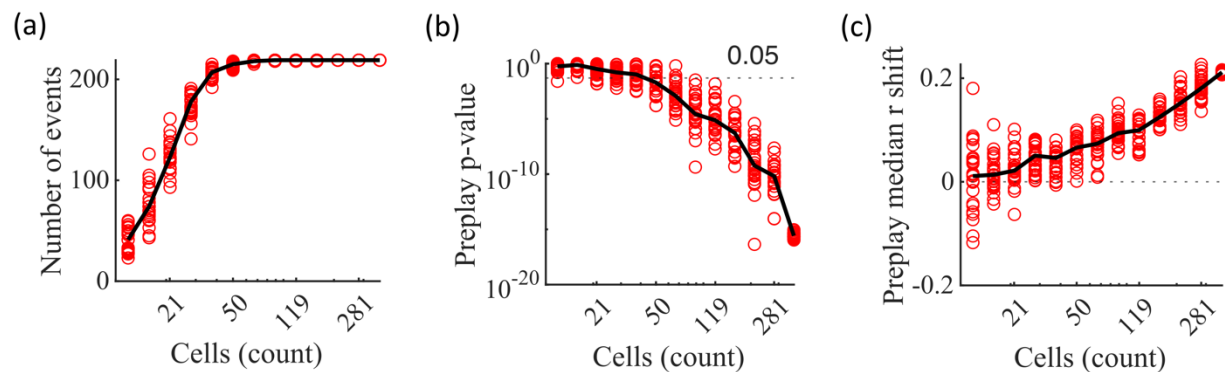
Figure 4—figure supplement 1: Example preplay events from the Shin et al., 2019 data

1075

1076 Example preplay events. Same as Figure 2f but for events from the hippocampal data from
1077 Shin et al., 2019. The height of each plot spans the length of the trajectory used for
1078 decoding, divided into 2 cm spatial bins. The width of each plot spans the duration of the
1079 detected event, divided into 10 ms time bins. Probability is shown in color.

1080

1081



1082

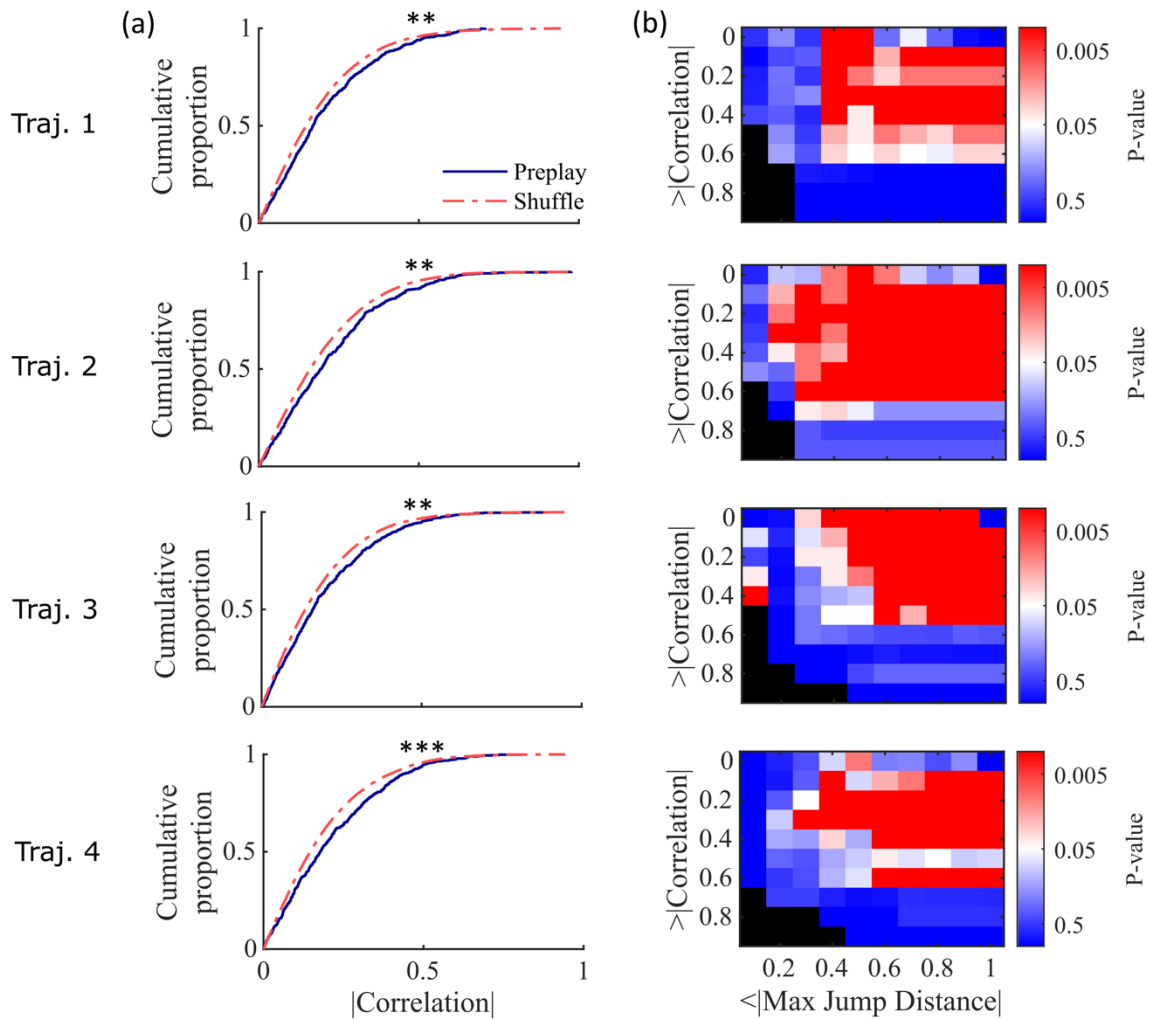
Figure 4—figure supplement 2: Significant preplay can typically be identified with as few as 50 cells

1083

1084 **(a-c)** Results from performing the same Bayesian decoding on the same simulated
1085 population burst events (PBEs) in Figure 4c but using only random subsets of the
1086 excitatory cells for performing the decoding analysis. Each circle is the result of an analysis
1087 performed on one random subset of the cells. 25 random subsets were analyzed for each
1088 analyzed cell count. The subset sizes are logarithmically spaced. Black lines show the
1089 median value. The variability at N=375 is due to the variation in the randomness of the
1090 time-bin shuffles. **(a)** Number of events meeting the inclusion criterion for decoding
1091 analysis. **(b)** P-value of the KS-test comparing actual vs shuffled event absolute weighted
1092 correlations. A majority of the random subsets of 50 cells (17 out of 25) produce preplay p-
1093 values below 0.05. **(c)** Shift in the median absolute weighted correlation of actual events
1094 relative to shuffled events.

1095

1096



1097

Figure 4—figure supplement 3: Preplay statistics by trajectory for Shin et al., 2019 data.

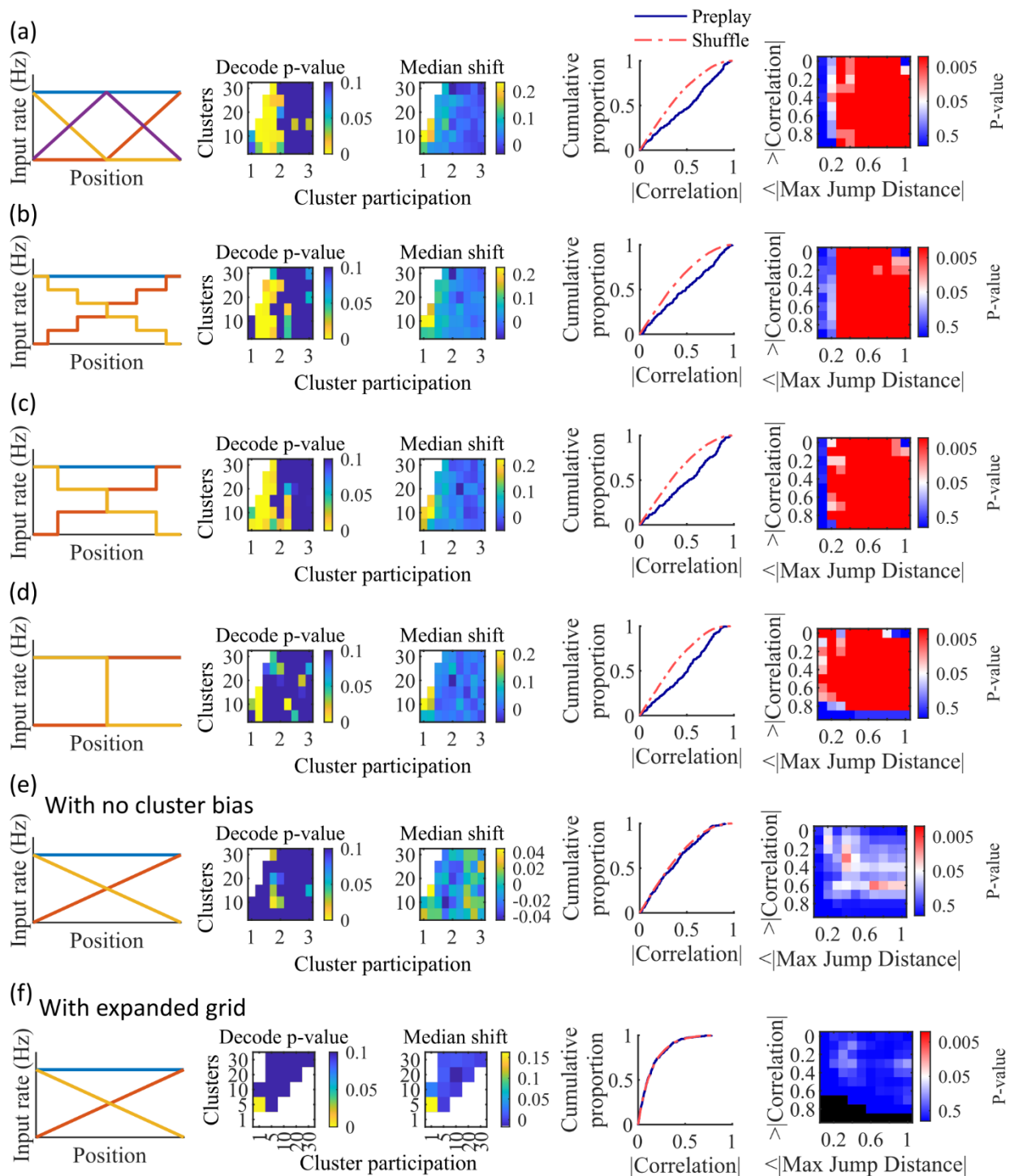
1098

1099

(a) Same as Figure 4a but separated by results from decoding by each of the 4 trajectories of the W-track individually (trajectory 1, center arm to right arm; trajectory 2, right arm to center arm; trajectory 3, center arm to left arm; trajectory 4, left arm to center arm). KS-test for each trajectory: trajectory 1, $p=0.0030$; trajectory 2, $p=0.0028$; trajectory 3, $p=0.0027$; trajectory 4, $p=5.461 \times 10^{-5}$. ** $p < 0.01$, *** $p < 0.001$. (b) Same as Figure 4b but separated by results from decoding by each of the 4 trajectories individually.

1105

1106



1108 **Figure 4—figure supplement 4: Additional simulations support the consistency and**
 1109 **robustness of the model to variations in spatial input forms.**

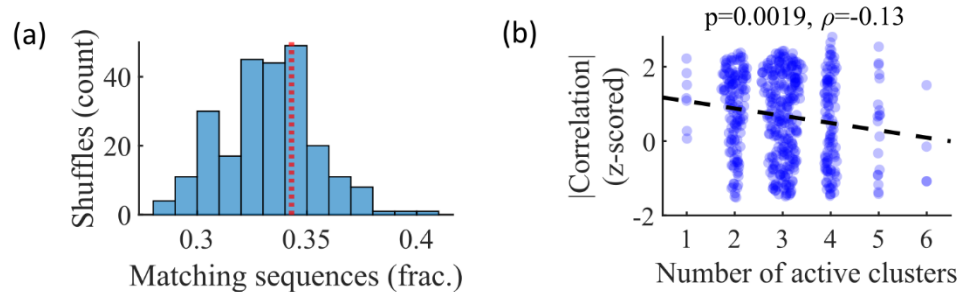
1110 Each row corresponds to a different parameter grid simulation, with statistics calculated as
 1111 in the corresponding panel from Figure 4. (a) Preplay statistics are similar to the main

1112 simulation results when a third linearly varying spatial cue is included in the inputs to the
1113 network (CDF KS-test, $p=3.9e-13$, KS-statistic=0.26). **(b)** Preplay statistics are similar to the
1114 main simulation results when a stepped input is used (CDF KS-test, $p=2.5e-08$, KS-
1115 statistic=0.20). The stepped input is less spatially informative since stretches of adjacent
1116 locations on the track have identical spatial input. **(c)** Same as (b), but with three step
1117 increments (CDF KS-test, $p=6.2e-13$, KS-statistic=0.26). **(d)** Same as (c), but with a single
1118 step increment (CDF KS-test, $p=4.9e-13$, KS-statistic=0.26). With this input the fiducial
1119 parameter set still shows significant preplay (right two columns), but most of the
1120 parameter grid loses significant preplay. **(e)** When the bias in cluster spatial input location
1121 is removed preplay is no longer significant (CDF KS-test, $p=0.34$, KS-statistic=0.063). **(f)** A
1122 parameter grid that shows greater values of cluster participation do not have significant
1123 preplay. Values along the diagonal where clusters equals cluster participation are
1124 equivalent to a random cluster-less network. Example parameter point is at clusters=5 and
1125 cluster participation=5 (CDF KS-test, $p=0.99$, KS-statistic=0.02).

1126

1127

1128



1129 **Figure 5—figure supplement 1: Relationship between cluster activation and preplay.**
1130 **(a)** Out of all events from the fiducial parameter set simulations where 3 unique clusters
1131 were active, the fraction of those events with sequences that match the order of cluster
1132 biases on the track (red line) is consistent with the values expected by randomly sampling
1133 clusters (blue). **(b)** Z-scored absolute weighted preplay correlation is negatively correlated
1134 with the number of active clusters (Spearman's rank correlation).

1135